Environmental Modelling & Software 102 (2018) 39–48

Contents lists available at ScienceDirect

Environmental Modelling & Software

journal homepage: www.elsevier.com/locate/envsoft

Simulating eroded soil organic carbon with the SWAT-C model

Xuesong Zhang [a, b, *]

[a] Joint Global Change Research Institute, Pacific Northwest National Laboratory, University of Maryland, College Park, MD, 20740, USA
[b] Earth System Sciences Interdisciplinary Center, University of Maryland, MD, 20740, USA

ARTICLE INFO

Article history:
Received 16 November 2017
Received in revised form
5 January 2018
Accepted 7 January 2018
Available online 24 January 2018

Keywords:
Agriculture
Greenhouse gases
Erosion
Soil organic carbon

ABSTRACT

The soil erosion and associated lateral movement of eroded carbon (C) have been identified as a possible mechanism explaining the elusive terrestrial C sink of ca. 1.7–2.6 PgC yr^{-1}. Here we evaluated the SWAT-C model for simulating long-term soil erosion and associated eroded C yields. Our method couples the CENTURY carbon cycling processes with a Modified Universal Soil Loss Equation (MUSLE) to estimate C losses associated with soil erosion. The results show that SWAT-C is able to simulate well long-term average eroded C yields, as well as correctly estimate the relative magnitude of eroded C yields by crop rotations. We also evaluated three methods of calculating C enrichment ratio in mobilized sediments, and found that errors associated with enrichment ratio estimation represent a significant uncertainty in SWAT-C simulations. Furthermore, we discussed limitations and future development directions for SWAT-C to advance C cycling modeling and assessment.

Software availability

Software: SWAT-C
Developer: Xuesong Zhang
Operating systems: Windows & Linux
Dependent software: FORTRAN 90
Availability: Free of charge; SWAT-C has been released at http://swat.tamu.edu/software/swat-executables within the latest version of SWAT. The new code revision regarding eroded C yields calculation and enrichment ratio estimation will be released to the public through the SWAT website.

1. Introduction

Accurate quantification of carbon (C) cycling in the Earth system is crucial for effective development of science-based decision tools and management strategies aimed at reducing C emissions. Current estimates of global CO_2 fluxes consistently infer a missing terrestrial C sink (also known as "residual terrestrial" or "land" sink) of 1.7 and 2.6 Pg C yr^{-1} for the 1980s and 1990s, respectively (IPCC, 2013). This residual sink is comparable in magnitude to other major components of the global C budget (e.g. the net ocean uptake of ca. 2.3 Pg C yr^{-1} or C emissions of ca. 1.0 Pg C yr^{-1} from land use change) (Ciais et al., 2014). A possible mechanism contributing to this missing sink is the soil erosion processes, which may induce a global C sink of ~0.12–1.5 PgC yr^{-1} (Smith et al., 2001; Stallard, 1998; Van Oost et al., 2007; Quinton et al., 2010). However, the C dynamics across terrestrial-aquatic interfaces, regulated by both biotic and abiotic processes across various temporal and spatial scales, remain poorly characterized. Given the magnitude and the degree of uncertainty associated with the erosion-induced C sink, there is an urgent need to elucidate its causes and mechanisms in order to avoid unexpected consequences when developing and deploying C management strategies and policies (Houghton, 2002).

Soil erosion and lateral movement of sediment and nutrients from land to waters not only modify soil quality but also alter terrestrial biogeochemical cycles (Lal, 2004; Liu et al., 2003; Berhe et al., 2007). Soil erosion laterally redistributes and removes soil organic carbon (SOC) and other nutrients across terrestrial landscapes. Global estimates of SOC erosion fluxes have varied widely from 0.5 to 6.0 Pg C yr^{-1} (Lal, 2003; Van Oost et al., 2007; Müller-Nedebock and Chaplot, 2015). Process-based terrestrial ecosystem modeling framework based on the CENTURY terrestrial C model (Parton et al., 1994) have been developed and tested for quantifying SOC erosion and associated biogeochemical processes (Harden et al., 1999; Liu et al., 2003; Izaurralde et al., 2007). Additionally, the soil erosion critically impacts trophic states as well as C stocks and flows in aquatic ecosystems (Cole et al., 2007; Tranvik et al.,

* Joint Global Change Research Institute, Pacific Northwest National Laboratory, University of Maryland, College Park, MD 20740, USA.
E-mail addresses: Xuesong.zhang@pnnl.gov, xzhang14@umd.edu.

https://doi.org/10.1016/j.envsoft.2018.01.005
1364-8152/

2009; Battin et al., 2009; Tank et al., 2010). Soil erosion mobilizes and introduces large amounts of particulate organic carbon (POC) from upland landscapes into streams, rivers, and reservoirs, where POC undergoes complex transport and transformation processes; POC not consumed in inland waters is transported by rivers to estuarine and coastal ecosystems (Hope et al., 1994), where it could be buried, biogeochemically transformed, or returned back to the atmosphere as CO_2 (Bauer and Bianchi, 2011). C transport and transformation processes link C cycling across terrestrial and aquatic ecosystems at the watershed scale and represent an important component of the boundless global C cycle (Battin et al., 2009), but has not been well understood and characterized (Trimmer et al., 2012).

Multiple field scale soil erosion models are available. The empirically-based Universal Soil Loss Equation (USLE) (Wischmeier and Smith, 1978; Wischmeir, 1965) is a field scale model that is capable of simultaneously considering multiple soil erosion control factors, such as surface cover, terrain characteristics, precipitation, and conservation practices. Based on the USLE model, multiple revised methods have been proposed and widely adopted, such as Revised USLE (RUSLE) by Renard et al. (1991) and Modified USLE (MUSLE) by Williams and Berndt (1977). More physically based soil erosion models (Jetten et al., 1999; Nearing et al., 2005), such as Water Erosion Prediction Project (WEPP) (Nearing et al., 1989), KINematic runoff and EROSion (KINEROS) (Woolhiser et al., 1990), EUROpean Soil Erosion Model (EUROSEM) (Morgan et al., 1998), and Plot Soil Erosion Model 2D (PSEM_2D) (Nord and Esteves, 2005), have been developed to explicitly represent detachment and transport processes during soil erosion (Ellison, 1947). Previous studies showed that field scale soil erosion modeling is subjective to multiple errors sources (Jetten et al., 1999; Nearing et al., 2005; Nord and Esteves, 2005), such as input data quality, user's choices in preparing input data, and inherent errors from simplified representation of the soil processes; often the importance of different uncertainty sources varies by models and experimental data employed. In general, the physically based models require more detailed spatial data and finer execution time step (e.g. minutes), and are often event based. A comparison of field scale soil erosion models (Jetten et al., 1999) showed that empirically models do not underperform physically models for long-term continuous simulations. Given the availability of terrain, climate and management data and the purpose of linking erosion with SOC losses for long-term simulations, we chose the MUSLE soil erosion model.

In addition, the MUSLE has been incorporated within the SWAT model (Arnold et al., 1998), which is a widely used process-based watershed model for reproducing observed hydrologic and/or pollutant loads across a wide range of watershed scales and environmental conditions, as well as for assessing impacts of conservation practices, land use, climate change, water management, and other scenarios (Gassman et al., 2007). Using MUSLE within the SWAT framework will greatly benefit future efforts to understand the fate of eroded sediments and C in downstream aquatic ecosystems and assess watershed scale C balance. Furthermore, in recognition of the need of a coupled watershed scale C cycling model, recent efforts (Yang and Zhang, 2016; Yang et al., 2017; Zhang et al., 2013b) enhanced and tested SWAT for simulating carbon dioxide (CO_2) and nitrous oxide (N_2O) fluxes of diverse upland ecosystems (referred to as SWAT-C hereafter). The revised coupled C, nitrogen and phosphorus cycles in SWAT-C are derived from three agroecosystem models, including the CENTURY model (Parton et al., 1994) and its daily version (DAYCENT) (Del Grosso et al., 2001), the Environmental Policy Integrated Climate (EPIC) model (Williams, 1990; Izaurralde et al., 2006), and the Decision Support System for Agrotechnology Transfer model (DSSAT) (Jones et al., 2003; Gijsman et al., 2002), as described in Zhang et al. (2013b). Wu et al. (2016) also explored the joint use of SWAT and DAYCENT to assess carbon dynamics. The SWAT-C model's C module has been tested for simulating CO_2 fluxes at 16 eddy covariance flux towers (Yang and Zhang, 2016; Zhang et al., 2013b). Those efforts lay a solid foundation for linking terrestrial C cycling with soil erosion.

Here, the major objective of this study is to test SWAT-C for simulating long-term sediment and eroded C using the long-term measurements from a small watershed (W118) in the North Appalachian Experimental Watershed (NAEW) research station (Hao et al., 2001). The outcome resulting from this study is expected to help understand the strength and weaknesses of SWAT-C for predicting the lateral movement of C from cropland into adjacent water bodies, thereby supporting its future development and applications to help understand C cycling across terrestrial and aquatic ecosystems.

2. Materials and methods

2.1. Description of the SWAT-C model

The SWAT model is a continuous, long term, distributed-parameter hydrologic model, which has been incorporated into the U.S. Environmental Protection Agency (US EPA) Better Assessment Science Integrating Point & Nonpoint Sources (BASINS) software package (Luzio et al., 2002), and is also being considered as a core watershed model by the United States Department of Agriculture (USDA) for applications in the Conservation Effects Assessment Project (CEAP) (Richardson et al., 2008) across watersheds in the U.S. For a watershed application, SWAT subdivides a watershed into subbasins connected by a stream network, and further delineates Hydrologic Response Units (HRUs) consisting of unique combinations of land cover and soils in each subbasin. For each HRU, SWAT simulates surface and subsurface flow, evapotranspiration, soil moisture sediment generation, carbon and nutrient cycling, and plant growth and development (Neitsch et al., 2011). The plant growth processes in SWAT are based on the EPIC model, which uses a revised version of Crop Environment REsource Synthesis (CERES) (Williams et al., 1989; Jones et al., 1991) and employs the concept of radiation-use efficiency by which a fraction of daily photosynthetically-active solar radiation is intercepted by the plant canopy and converted into plant biomass. Daily gains in plant biomass are affected by vapor pressure deficits, atmospheric CO_2 concentrations, nutrients availability, and other environmental controls and stresses.

In the SWAT-C version (Zhang et al., 2013b), following the CENTURY model (Parton et al., 1994), the soil organic matter (SOM) and residue are represented with five pools. Plant litter is divided into the easily decomposable metabolic (e.g. proteins and sugars) and recalcitrant structural (e.g. lignin and cell walls) component. An active microbial biomass pool that has a turnover of months to a few years, including soil microbes and microbial products. The slow humus pool receives C and N from the decomposition of structural litter, metabolic litter, and microbial biomass and often has a turnover time of 20–50 years. The most recalcitrant SOM lies in the passive humus pool, which includes physically and chemically stabilized SOM sorbed to clays with long turnover times (400–2000 years) (Parton et al., 1993, 1994). In addition to substrate specific properties, the decomposition and transformation of structural litter, metabolic litter, passive humus, slow humus, and microbial biomass are also influenced by abiotic factors, such as soil temperature, soil water content, tillage enhancement, oxygen availability, and soil texture (Parton et al., 1994; Gijsman et al., 2002; Izaurralde et al., 2006).

SWAT-C simulates soil erosion using the modified universal soil

loss equation (MUSLE) (Williams and Berndt, 1977). Eroded SOC loss is derived by multiplying the amount of eroded soil with the concentration of SOC in mineral soils and an enrichment ratio. The MUSLE is a variant of the equation Universal Soil Loss Equation (USLE) (Wischmeier and Smith, 1978; Wischmeir, 1965) and is represented in the following form:

$$sed = 11.8 \cdot \left(Q_{surf} \cdot q_{peak} \cdot area_{hru}\right)^{0.56} \cdot K_{USLE} \cdot C_{USLE} \cdot P_{USLE} \cdot LS_{USLE} \cdot CFRG \quad (1)$$

where *sed* is the sediment yield on a given day (Mg), Q_{surf} is the surface runoff volume (mm H_2O ha^{-1}), q_{peak} is the peak runoff rate (m^3 s^{-1}), $area_{hru}$ is the area of the HRU (ha), K_{USLE} is the USLE soil erodibility factor that is determined by sand, clay, silt, and organic C content, C_{USLE} is the USLE cover and management factor (dimensionless), P_{USLE} is the USLE support practice factor (dimensionless), LS_{USLE} is the USLE topographic factor (dimensionless), *CFRG* is the coarse fragment factor (dimension less). C_{USLE} is land cover specific, with grassland having smaller values than row crops. Residue collection influences this factor by reducing surface cover, leading to more erosion.

The concentration of SOC in eroded mineral soils is a product of the concentration of SOC in top soil and an enrichment ratio. We further use the following equation to calculate the amount of eroded SOC:

$$sedC = sed \cdot conc_{soc,soil} \cdot ER \quad (2)$$

where *sedC* is the eroded C yield on a given day (Mg), $conc_{soc,soil}$ is the fraction of SOC in the top soil layer where eroded sediment comes from, *ER* is the ratio of the concentration of organic C transported with the sediment to the concentration in the soil surface layer. In the experimental site, measured *ER* was 1.7 (Hao et al., 2002), which was assumed to be fixed over time in the simulation study.

2.2. Enrichment ratio calculation

As smaller particles weigh less and are more easily transported than coarser particles, the sediment load to streams often has a greater proportion of clay sized particles or enriched in clay particles. SOM is attached primarily to colloidal (clay) particles, so the sediment load will also contain a greater proportion of concentration of organic C than that found in the soil surface layer. In SWAT, the enrichment ratio is estimated using the following empirical formula:

$$ER = 0.78 \cdot \left(conc_{sed,surf}\right)^{-0.2468} \quad (3)$$

where $conc_{sed,surf}$ is the concentration of sediment in surface runoff (Mg m^{-3} H_2O).

Our initial assessment of the default SWAT enrichment ratio calculation equation (Eq. (3)) showed that it estimated much higher *ER* than those reported in literature that are <3 in most cases Menzel (1980). This finding led us to examine other *ER* calculation options that have been derived from previous field experimental data. Here two equations are selected to understand uncertainties associated with *ER* calculation and subsequent implications for eroded C simulations. Based on multiple experimental data, Menzel (1980) derived a generalized equation that is hoped to hold for a wide range of vegetation and soil conditions:

$$ER = 7.4 \cdot (sedu)^{-0.2} \quad (4)$$

where *sedu* is sediment yield per unit area (kg ha^{-1}). This relationship has been widely used in nonpoint source pollution models, such as the Chemicals, Runoff, and Erosion from Agricultural Management Systems (CREAMS) (Knisel, 1980), to calculate nutrient enrichment ratios.

Wang et al. (2013) derived a SOC enrichment ratio relationship based on field rainfall simulation experiments in the Loam Belt area in Central Belgium:

$$ER = 2.46 * e^{-0.065 \cdot SC} + 1.0 \quad (5)$$

where *SC* is sediment concentration in surface runoff with a unit of (g L^{-1} H_2O).

2.3. Description of the experimental site

The experimental site is a small watershed (W118) located within the USDA's NAEW research station (40°22′ N, 81°48′ W) near Coshocton, Ohio, which was established in 1938 to study runoff, erosion, and water quality as influenced by varying agro-ecosystems under different crop covers and management practices. More detailed description of the study site and its location is provided by Owens et al. (2010). The study area receives long-term annual average precipitation of 937 mm (1951–1998), with a standard deviation of 49.9 mm. On average, Spring (April, May and June) and summer (July, August, and September) receive 283.1 mm and 269.2 mm precipitation, respectively. In contrast, precipitation is less in autumn (October, November, and December) and winter (January, February, and March), which is 185.9 mm and 200.1 mm, respectively. Annual average daily air temperature is above 16.0 °C, with average daily maximum air temperature of 16.0 °C and average daily minimum air temperature 3.4 °C. The W118 watershed covers an area of 0.79 ha, and has a slope gradient of 10% with the slope length of 132 m. The sediment and eroded C transported by surface runoff were collected at the outlet of the small catchment to determine the yields of sediment and eroded C (Hao et al., 2001). The dominant soil type of the watershed is silt loam (Kelly, 1975).

Historical cropping systems have been described in Hao et al. (2001), Kelly (1975), Shipitalo and Edwards (1998) and in Owens and Edwards (1993), and can be grouped into four major phases. The first phase is between 1951 and 1970 with a four year rotation of plow tilled corn (*Zea mays* L.)- winter wheat (*Triticum aestivum* L.)-meadow-meadow (CWMM). For corn years, soils were plowed with moldboard, disk (twice), and harrow (once) before planting in late April or early May, and a rate of 56 kg ha^{-1} fertilizer (5-20-20) that contains 5% nitrogen-20% phosphorus-20% potash and 9 Mg ha^{-1} cattle manure was applied or plowed into the soil. Corn harvesting occurred in early October, with corn stover chopped and spread on the field. For winter wheat, soils were disked before drilling the seeds, and planting date is within 2 weeks from corn harvest. Winter wheat received a fertilization rate of 112 kg ha^{-1} fertilizer (5-20-20) and was harvested in next year's early July. For the two meadow years, hay harvesting occurred twice in late June and early August, respectively. The second phase (1971–1975) experienced plow tilled continuous corn (CC) (except no-till corn in 1974). During this period, soil amendments included N fertilizer of 225 kg ha^{-1} of urea or NH_4NO_3 applied in spring and phosphorous applied in fall to reduce nutrient stress on plant growth. The third phase (1976–193) is continuous Meadow with no-till and twice harvesting in late June and early August, respectively. The fourth phase is between 1985 and 1998, planted with a no-till corn and

soybean (*Glycine max (L.) Merr.*) rotation (CS). During this phase, corn received N fertilizer of 225 kg ha^{-1} of urea or NH_4NO_3 applied in spring and phosphorous applied in fall. In general corn and soybean were planted in late April or early May, and harvested October. Residues from corn and soybean are left intact on ground surface. Contour farming was adopted for row crops.

2.4. Model evaluation

Moriasi et al. (2007) reviewed and summarized multiple evaluation metrics used in model skill assessment. Here we selected three widely used descriptive statistics that has been widely used for evaluating performance of the SWAT model. The first metric is percent bias (*PBIAS*) (Gupta et al., 1999) calculated as:

$$PBIAS = \left(\frac{\sum_{k=1}^{T}(f_k - y_k)}{\sum_{k=1}^{T} y_k} \right) \times 100 \quad (6)$$

where f_k is the model simulated value at a time unit or location k, y_k is the corresponding benchmark data value, and T represents the total pairs of data. *PBIAS* measures the average tendency of the simulated data to be larger or smaller than their observed counterparts. Small *PBIAS* values means less model bias.

The second metric is coefficient of determination (R^2) (Legates and McCabe, 1999):

$$R^2 = \left\{ \frac{\sum_{k=1}^{T}(y_k - \bar{y})\left(f_k - \bar{f}\right)}{\left[\sum_{k=1}^{T}(y_k - \bar{y})^2\right]^{0.5}\left[\sum_{k=1}^{T}\left(f_k - \bar{f}\right)^2\right]^{0.5}} \right\}^2 \quad (7)$$

where $\bar{y}$ is the mean of observed data for the entire time period or across all sites under evaluation, $\bar{f}$ is the mean of simulated data. The other symbols are the same as defined above. R^2 ranges between 0.0 and 1.0 and represents the proportion of the total variance in the observed data that is explained by the model. The higher the R^2 values, the better the model performance.

The third metric is Nash-Sutcliffe efficiency (E_{ns}) (Nash and Sutcliffe, 1970):

$$E_{ns} = 1.0 - \frac{\sum_{k=1}^{T}(y_k - f_k)^2}{\sum_{k=1}^{T}(y_k - \bar{y})^2} \quad (8)$$

all symbols are the same as those introduced above. E_{ns} indicates how well the plot of the observed value versus the simulated value fits the 1:1 line, and ranges from $-\infty$ to 1.

3. Results and discussion

3.1. Comparison between simulated and observed long-term sediment and eroded carbon yields

With a fixed *ER* value of 1.7, we simulated annual sediment and eroded C yields over the period of 1951–1998 (Fig. 1). Averaged over 1951–1998, SWAT-C slightly underestimated sediment yield by 14%, with the simulated average of 1.03 Mg ha^{-1} yr^{-1} vs. the observed average of 1.2 Mg ha^{-1} yr^{-1} (Fig. 2). For eroded C, SWAT-C simulated value of 0.022 Mg C ha^{-1} yr^{-1} was 29% lower than the observed value of 0.031 Mg C ha^{-1} yr^{-1}. The time series plots in Fig. 1 also showed that SWAT-C captured well the overall temporal pattern of sediment and eroded C yield over the simulation period. In particular, SWAT-C captured years with the highest and second highest yields of sediment of 19.7 and 7.63 Mg ha^{-1} yr^{-1}, respectively, but with less magnitude. Similarly, we found SWAT-C also

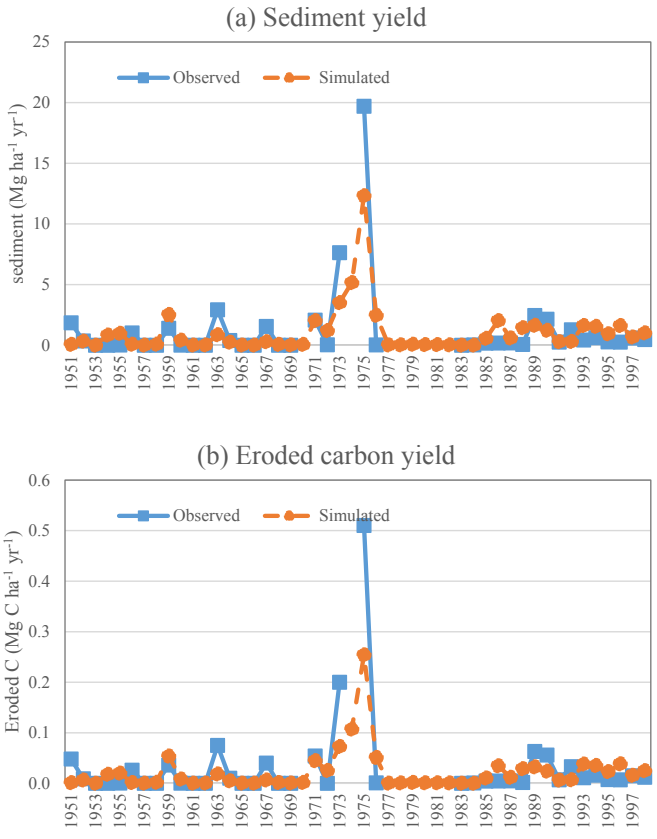

Fig. 1. Simulated and observed annual sediment (a) and eroded C (b) yield for the period of 1951–1998. Simulated values are derived by SWAT-C with a fixed enrichment ratio of 1.7 as derived from measured data by Hao et al. (2001).

reproduced the peak eroded C yield during those two years. Overall, the high coefficient of determination values for both simulated sediment and eroded C yields (0.85 and 0.84, respectively) indicate the capability of SWAT-C to explain temporal variability of lateral flow of sediment and eroded C over a long period. However, the E_{ns} values of 0.70 and 0.61 for sediment and eroded C yields simulations showed that there are noticeable different between the simulated and observed magnitude of the variables of interests at the annual time step.

Further examination of individual years' sediment and eroded C yields revealed larger uncertainties of SWAT-C simulations at the annual time scale. For example, SWAT-C underestimated sediment and eroded C yields by −37% and −50%, respectively, for year 1975. For year 1973, the *PBIAS* values were −54% and −63%, respectively, for sediment and eroded C yields. Summarized over the 41 years with observations, SWAT-C prediction error was larger than 50% for 29 years for both sediment and eroded C yields simulations. When the two years with highest sediment yields are removed, the R^2 values decreased to 0.09 and 0.08, respectively, for sediment and eroded C simulations. This finding indicates the high uncertainty of using SWAT-C to predict sediment and eroded C yield for a specific year, which may be caused by numerous factors related to characterizing biophysical and biogeochemical processes within an agricultural field.

SWAT-C uses SOC content in the top 10 mm soils and enrichment ratio to estimate C concentration in sediment, therefore, in Table 1 we also listed the simulated top 10 mm SOC content to show the variation in SWAT-C performance for different crop rotations. Due to the lack to observations for the top 10 mm, we could not directly assess SWAT-C's performance for this top layer. But in

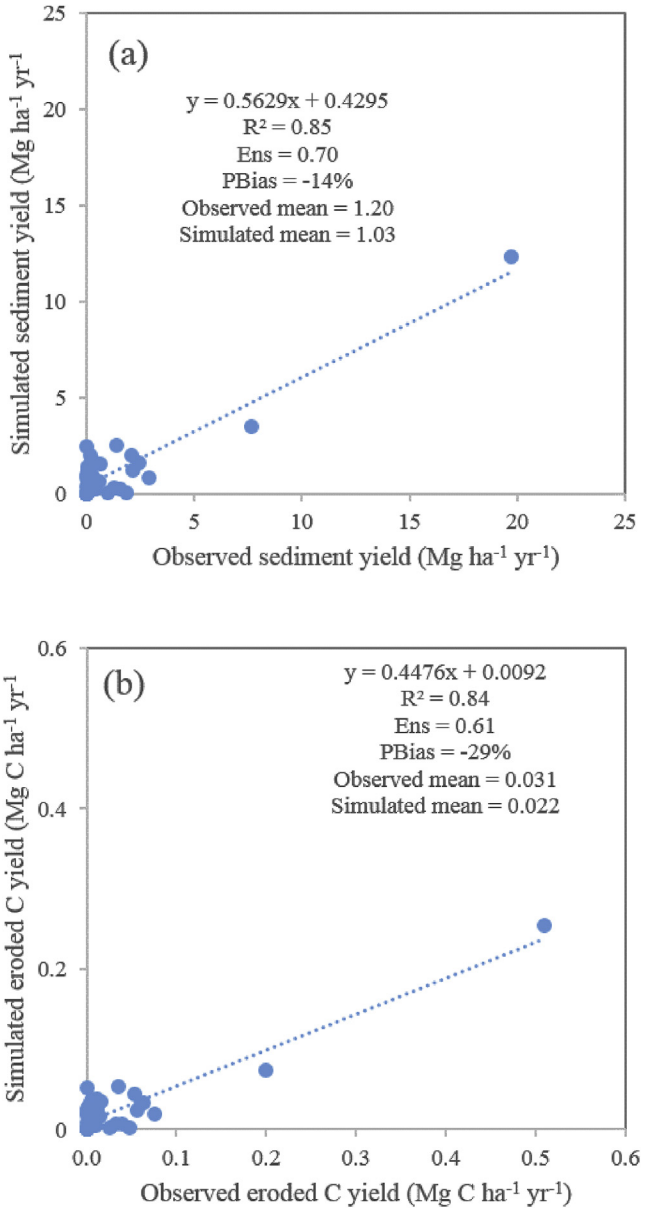

Fig. 2. Scatter plots of simulated and observed annual sediment (a) and eroded C (b) yield for the period of 1951–1998. Descriptive statistics, including observed and simulated mean values, coefficient of determination, Nash-Sutcliffe efficiency and percentage of bias, are also shown on the graph.

combination with the simulations of eroded C for the four crop rotations, we will discuss the potential implications of top 10 mm SOC estimation for explaining bias in simulated eroded C in the following section 3.2.

In addition to reasonable reproduction of long-term eroded C, SWAT-C was assessed for simulating SOC stocks over the simulation period (Table 1). SWAT-C correctly simulated the direction of the change of SOC storage in the top 30 cm soils, but over-predicted the magnitude by 1.1 Mg C ha^{-1} over the 48 years period. A closer look at the predicted SOC stocks by soil depth indicated that SWAT-C overestimated the changes of SOC in the top 0–10 cm and 10–20 cm soil horizons, but underestimated the SOC change in the soil depth between 20 and 30 cm. Although both observed data and SWAT simulations show increases in the top 0–10 cm, the magnitude of observed increase was 0.5 Mg C ha^{-1} which is much lower than the simulated increase of 3.6 Mg C ha^{-1}. In contrast, for SOC in 20–30 cm soil horizons, SWAT-C simulated a decrease of 0.53 Mg C ha^{-1}, while observed values indicate an increase of 2.5 Mg C ha^{-1}. For the 10–20 cm soil horizon, both SWAT-C and observed values showed a decrease in SOC storage over the simulation period.

SWAT-C was able to simulate responses of SOC storage to different crop rotations (Table 1). As the lack of SOC observations, we could not give direct assessment of the accuracy of simulated SOC storage under these four crop rotations. In general, it seems reasonable that the two rotations with meadow exhibited higher SOC in deeper soil layers than the CC-PT and CS-NT rotations, given that perennial grasses have deeper root and higher root-shoot ratio than annual crops (Zhang et al., 2011).

In general, SWAT-C predictions matched well the total SOC storage in the 0–30 cm soil depths. Note that there was noticeable difference in simulated and observed SOC for each soil layer. The mismatch between the SWAT-C simulated and observed SOC stocks may be caused by uncertainties from different sources. The first source of uncertainty arises from the uncertainties associated with the SOC measurements. Measurements taken at different locations within a field vary from each other due to spatial heterogeneity (Hoffmann et al., 2014). Often multiple replicate measurements were taken to estimate uncertainties arising from spatial heterogeneity Hao et al. (2002), as illustrated by the ranges of SOC observations obtained at upper, middle and lower slope positions (Table 1). For example, the measured 0–30 cm SOC ranged between 33.3 and 39.0 Mg C ha^{-1}. The range of SOC values were derived through repeated measurements at a limited number of locations within the agricultural fields, which are unlikely to reliably to represent total uncertainty caused by soil spatial heterogeneity (Donovan, 2012). In addition, accuracy of SOC measurements suffers from uncertainties in soil bulk density determination (Walter et al., 2016) and intrinsic limitations of SOC measurement tech-

Table 1
Simulated and observed SOC storage at different soil depths (Mg C ha^{-1}).

Soil depth	Observed Initial SOC[a]	CWMM-PT (1951–70)[c]	CC-PT (1971–75)[c]	M-NT (1976–83)[c]	CS-NT (1984–98)[c]	Observed final SOC[b]
0-10 mm	N/A	1.2	0.9	0.8	2.9	N/A
0-10 cm	17.6	16.3	15.9	16	21.2	18.1 (16.1–19.3)
10-20 cm	13.9	16.1	17.3	16.3	13.2	12.3 (12.1–12.6)
20-30 cm	4	4	3.9	4	3.47	6.5 (5.0–7.5)
0-30 cm	35.6	36.5	37.1	36.3	37.9	36.8 (33.3–39.0)

[a] Initial SOC represents SOC stocks in 1951.
[b] Represents average SOC stocks observed at the end of 1998 as reported by Hao et al. (2002) with the numbers in parentheses representing the range of observations at upper, middle and lower slope positions.
[c] SWAT-C simulated SOC stocks at the end of different crop rotations: 1951–1970: Corn-Wheat, Meadow-Meadow (CWMM) with Plow Till (PT); 1971–75: Continuous Corn (CC) with PT; 1976–1983: Meadow (M) with No-Till (NT); 1984–1998: Corn-Soybean (CS) with NT.

niques as discussed in Schumacher (2002) and Da Silva Dias et al. (2013).

The second type of uncertainties mainly lie in errors in model simulations. For example, errors associated with model inputs (e.g. climate forcing, soil properties, timing and characterization of each agronomic operations) can translate into errors in model simulations (Grosz et al., 2017). The uncertainties associated with SWAT's hydrologic and biogeochemical simulation algorithms (e.g. evapotranspiration, surface runoff, plant nutrient uptake, root development, and SOC decomposition) may influence water budget, plant cover, SOC dynamics and biogeochemical constituents (Zhang et al., 2014).

Although the uncertainties associated with field measurements and model simulations prevent us from achieving simulations that exactly match the observations, the statistical metrics (Fig. 2 and Table 1) show that SWAT-C can reasonably reproduce the average magnitude and temporal variable of long-term annual sediment and eroded C loads. Furthermore, SWAT-C simulated well the long-term average SOC stocks in the top 30 cm. But SWAT-C did not represent well the depth distribution of SOC changes, indicating that the below ground root development and vertical variation of controls on SOC dynamics await further examination and improvements.

3.2. Soil erosion and eroded C yield by crop management

The analysis in section 3.1 reveals the noticeable discrepancies at the annual scale between simulated and observed sediment and eroded C loads, although the long-term average was well reproduced. This result is not surprising as previous studies showed that SWAT-C was able to capture long-term characteristics of agro-ecosystems, but performed less at the annual time scale given large uncertainties associated with input data and imperfections of the numerical algorithms (Srinivasan et al., 2010; Zhang et al., 2013a). This finding led to a follow-up question: how do SWAT-C perform over an intermediate time scale that is coarser than annual but finer than overall average? Here we conducted further examination of SWAT-C performances by different crop rotations or types.

SWAT-C simulated sediment and eroded C yields matched the relative magnitude of observed data by crop rotation (Fig. 3). The CC-PT rotation exhibited the highest soil erosion and associated SOC losses. This result is consistent with previous studies that soil plowing disturbs soil surface and increases the risks of erosion (Devanand et al., 2006; LeDuc et al., 2016). SWAT-C underestimated the sediment and associated eroded C yields during the CC-PT rotation by 2.5 Mg ha^{-1} yr^{-1} than observed, which is the major reason causing the lower simulated sediment load by SWAT-C, as the 5-year total sediment yields disproportionately accounted for ca. 61% of the total sediment yields over the 48 years. In contrast to the plow tilled CC rotation, SWAT-C overestimated sediment yields during the no-till CS rotation. Collectively, SWAT-C estimates narrowed the effects of conversion of conventional tillage to no-till practices on soil conservation.

Similar to our sediment yield analysis, the patterns of eroded C yield by crop rotation illustrate that SWAT-C tended to overestimate eroded C losses for crop rotations with low sediment yields, while underestimate eroded C losses for crop rotations with high sediment yields. These two types of bias offset each other and resulted in relatively low errors for the entire period, but diminish the value of SWAT-C to distinguish the effects of crop rotations on sediment and eroded C losses.

Note that the PBIAS values in simulated yields are larger than those in simulated eroded C (Fig. 3c), indicating that SWAT-C consistently underestimated SOC concentration in sediment. In general, PBIAS values in simulated eroded C is consistently lower

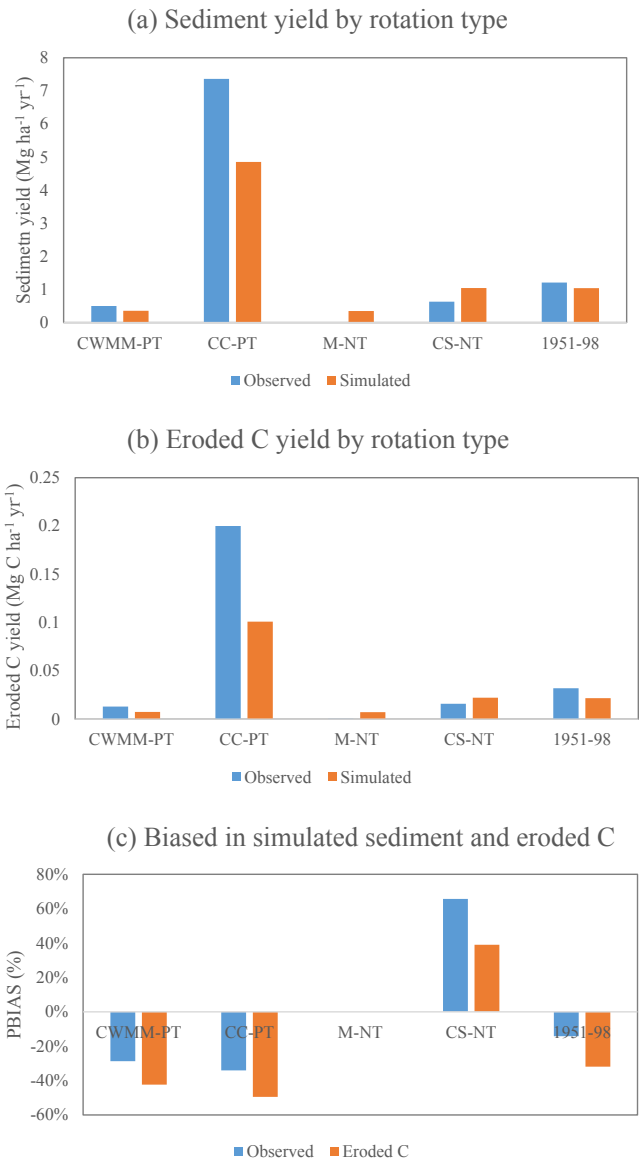

Fig. 3. Sediment and eroded C yields for different crop rotations. 1951–1970: CWMM-PT; 1971–75: CC-PT; 1976–1983: M-NT; 1984–1998: CS-NT.

than biased in simulated sediment yields by 13%–26% over the four assessment periods (Fig. 3c). Here, we excluded the M-NT period for analysis due to the large relative biases in SWAT-C simulated erosion under perennial grass cover. Assuming the fixed enrichment ratio derived from observations has little error, a possible explanation for this under-estimation of SOC concentration in sediment is that SWAT-C underestimated the 10 mm SOC. This finding calls for future examination of SWAT-C for simulating top 10 mm SOC against observations, which hold the potential to further improve eroded C simulations.

Further analyses by crop type show that SWAT-C underestimated sediment yields for corn and winter wheat, but overestimated sediment yields for soybean and meadow, as shown in Fig. 4. Similar patterns were obtained for SWAT-C simulated eroded C yields. It is worth noting that, for perennial grasses, SWAT-C estimates an average sediment yield of ca. 0.22 Mg ha^{-1} yr^{-1}, which was nearly10 times that of the observed 0.0027 Mg ha^{-1} yr^{-1}. As perennial grasses are believed to provide valuable soil conservation benefits, they have been widely promoted as a Conservation

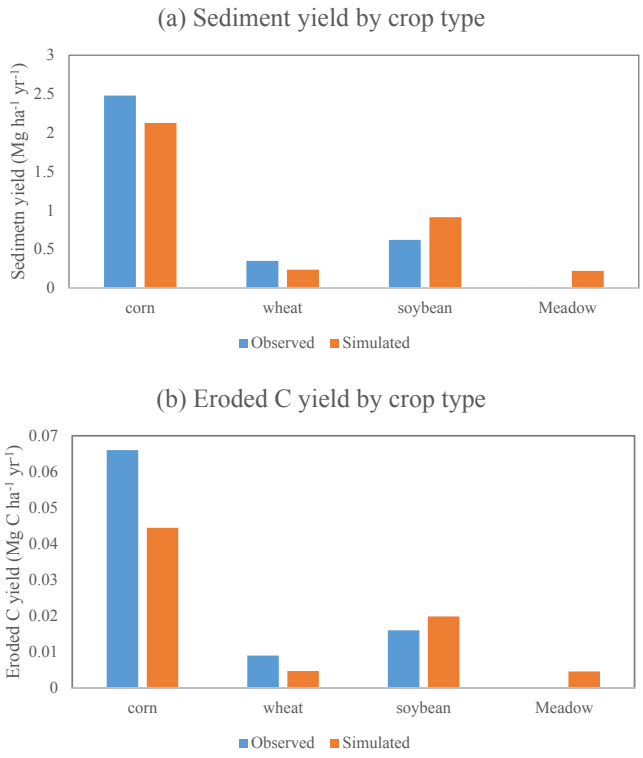

Fig. 4. Sediment and eroded C yields for different crop types.

Reserve Program (CRP) practice (LeDuc et al., 2016) and a promising source of cellulosic biomass to avoid food vs. biofuel conflict (Gelfand et al., 2013; Tilman et al., 2006). The overestimation of sediment yield and eroded C losses for meadow represent a weakness of SWAT-C to understand environmental benefits of perennial grasses.

3.3. Sensitivity of model simulations to different enrichment ratio calculation methods

Model simulations with different *ER* calculation methods reveal substantial variations in predicted *ER* values averaged over time, as well as in temporal *ER* patterns (Fig. 5a). In general, the default method in SWAT and the Menzel method overestimated *ER* values for most days, in particular for those days with small sediment yield or sediment concentration. This finding is in line with previous studies that showed larger uncertainties in *ER* values associated with storm events with low sediment yield or concentrations (Wang et al., 2013). Menzel (1980) also identified large uncertainties associated with *ER* estimations, and concluded that the Menzel method could over- or under-estimate within a factor of 5 for individual runoff events and within a factor of 2 for an annual average estimate. The *ER* values predicted by the Wang method matched well with the observed *ER* of 1.7, with slight overestimation for most days and noticeable underestimation for several years (e.g. 1971–1976).

Not surprisingly, the substantial difference in *ER* values predicted by different methods translated into the large discrepancy between simulated eroded C yields (Fig. 5b). However, the magnitude of difference between *ER* values is less than that between the eroded C yields (Table 2). For example, the average *ER* values derived by the Wang, Menzel, and Default equations were, respectively, 1.02, 3.07, and 3.97 times the observed *ER* of 1.7. In contrast, the eroded C yields predicted by the three methods were, respectively, 0.91, 1.38, and 1.88 times that predicted with the fixed *ER* of 1.7. The higher *ER* resulted in more depletion of SOC in the surface soil layer, therefore the increasing rate of eroded C yields is less than that of sediment yields in response to increases in *ER* values (Woods and Schuman, 1988).

3.4. Limitations and future directions

Based on the previous analyses, we identified the following limitations of SWAT-C that deserve future research to improve upon, in order to increase its credibility of representing the lateral flow of C that couples the terrestrial and aquatic ecosystem processes. A major limitation of this model assessment effort was that we did not have access to exact timing of crop management practices, which was shown to have significant impacts on the simulated C balance in previous site scale SWAT-C assessment (Zhang et al., 2013b). In addition, we used generic parameters in the SWAT database to characterize fertilization, tillage, and harvesting management practices. These settings may not represent well the site-specific conditions such as tillage depth, harvest index, and fertilizer application depth that influence surface residue cover, vertical SOC mixing and nutrient availability for SOC decomposition. Therefore, future assessment of SWAT-C at field sites with more detailed and accurate agronomic information would help better understand the strengths and weaknesses of SWAT-C to simulate the lateral movement of eroded C.

As discussed in section 3.1, SWAT-C captured the long-term average sediment and eroded C yields, but exhibited relatively large errors for individual year predictions. A possible reason is that the SWAT-C currently operates on a daily time step, preventing it from directly using hourly or sub-hourly precipitation to simulate peak flow. Given the significance of peak flow in the MUSLE equation based soil erosion estimation, the use of long-term statistical estimation of half-an-hour precipitation intensity makes it difficult for SWAT-C to accurately simulate rainfall event scale soil erosion and associated C losses. Recently, a physically based soil erosion calculation method was incorporated into SWAT (Jeong et al., 2011) that integrates features from (EUROSEM) and Areal Nonpoint Source Watershed Environmental Resources Simulation (ANSWERS) (Park et al., 1982). This method can be used to calculate hourly or subhourly soil erosion processes. In addition, the agricultural field was treated as a homogeneous unit, which ignores important effects of spatial variability on sediment detachment and deposition. For example, Hao et al. (2002) showed that C stocks differentiated greatly between the upper, middle and lower slope positions of the W118 experimental sites. SWAT is able to use a flexible configuration of upland landscapes (e.g. divide, hillslope, and floodplain) (Arnold et al., 2010), allowing for simulating the redistribution of sediment and SOC along the upland landscapes regulated by surface runoff carrying capacity and erosion/deposition processes. Further coupling between SWAT-C with the advanced landscape configuration functions within SWAT holds the potential to further improve eroded C erosion/deposition processes using refined precipitation data.

Based on the results in Figs. 2 and 3, the PBIAS values for simulated eroded C are lower than those for simulated sediment yields, with a difference between 13 and 26% for different crop rotations and assessment periods. For example, over the entire simulation period, the PBIAS is −14% and −29%, respectively, for sediment yields and eroded C estimation. These differences in PBIAS values indicate that uncertainties in simulated eroded C include both errors arising from sediment yield simulations and inherent errors in SOC algorithms. Given the lack of daily sediment

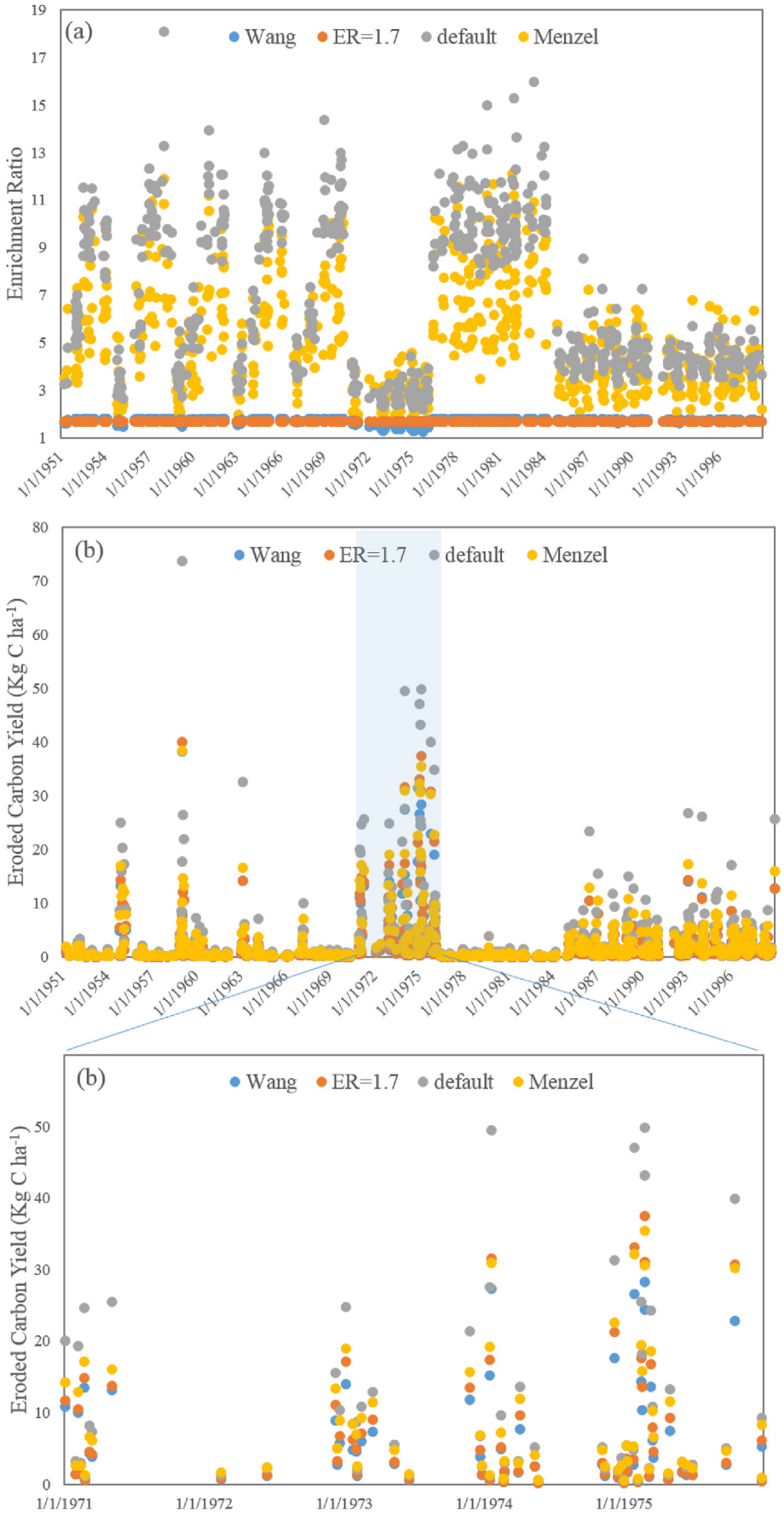

Fig. 5. Time series of predicted daily *ER* values (a) and eroded C yield (b) over those days with sediment yield $>10^{-6}$ Mg ha^{-1} day^{-1} with four different *ER* calculation methods. "ER = 1.7" denotes fixed *ER* value of 1.7 over time; "Wang" denotes the equation (5) by Wang et al. (2013); "Default" denotes the default *ER* calculation equation within SWAT; and "Menzel" denotes the equation (4) by Menzel (1980). In the plot of eroded C yields, the values below 0.000001 were not included to ensure legibility of the graph.

Table 2
Estimated ER and Simulated eroded C yield with different ER estimation methods.

ER method	ER = 1.7	Default	Wang	Menzel
Estimated ER	1.7	6.74	1.73	5.22
Simulated eroded C yield (Mg C ha^{-1} yr^{-1})	0.022	0.041	0.020	0.031

yield data to drive SWAT-C, we could not perform simulations to analyze potential implications of reducing sediment yield errors for improving eroded C estimation. However, such an exercise is valuable for better understanding sources of uncertainties in eroded C simulation, and await future research.

The large uncertainties associated with *ER* estimation deserve closer examination. The default *ER* calculation method within SWAT significantly overestimated observed *ER* values, and led to much overestimation of eroded C losses. Although the Wang method matched closely with the observed average *ER* values, it seems not able to represent variability of *ER* associated with individual rainfall-runoff events that have been demonstrated in previous field experiments (Wang et al., 2013). Using multiple *ER* equations to provide ensemble prediction may be a feasible option to estimate uncertainty in simulated eroded C yields. Evaluating more *ER* calculation methods against field data and identify the application conditions of each *ER* method will help choose the most appropriate method for a specific region or management conditions, thereby facilitating reducing uncertainty in eroded C predictions.

4. Conclusions

Soil erosion links terrestrial and aquatic ecosystem processes, and has been identified as an important process understudied for elucidating global/regional carbon cycles. In this study, we evaluated the SWAT-C model for simulating long-term annual sediment and eroded C yields at an experimental site within the NAEW research station. The results demonstrate the strengths of SWAT-C in reproducing long-term average eroded C yields and relative magnitude of eroded C yields by crop rotation or type. Noticeable biases were observed at the annual scale, which translated into the pronounced over- or under-estimation of eroded C yields by crop rotation or type. In general, SWAT-C overestimated eroded C losses for crop rotations or types with low sediment yields, while underestimated eroded C losses for crop rotations or types with high sediment yields. This weakness may cause SWAT-C to discount the environmental benefits of soil conservation practices. Based on the strengths and weaknesses of SWAT-C, we discussed future directions of further development of SWAT to better represent the lateral movement of eroded C, such as assessing more *ER* calculation methods and identifying each method's appropriate application contexts, and linking SWAT-C with advanced landscape configuration functions of SWAT to used physically based algorithms to represent soil erosion/sediment deposition processes. We anticipate the SWAT-C model assessment and development efforts presented here will help lay the foundation for a watershed tool to study watershed scale C cycling across terrestrial and aquatic ecosystems.

Acknowledgements

This work was funded by the NASA (NNX17AE66G) and USDA (2017-67003-26485 and 2017-67003-26484) Interagency carbon cycle science program, NASA's New Investigator Award (NNH13ZDA001N), and NSF INFEWS (1639327).

Appendix A. Supplementary data

Supplementary data related to this article can be found at https://doi.org/10.1016/j.envsoft.2018.01.005.

References

Arnold, J.G., Allen, P.M., Volk, M., Williams, J.R., Bosch, D.D., 2010. Assessment of different representations of spatial variability on SWAT model performance. Trans. ASABE 53, 1433–1443.
Arnold, J.G., Srinivasan, R., Muttiah, R.S., Willianms, J.R., 1998. Large area hydrologic modeling and assessment part 1:model development. J. Am. Water Resour. Assoc. 34, 73–89.
Battin, T.J., Luyssaert, S., Kaplan, L.A., Aufdenkampe, A.K., Richter, A., Tranvik, L.J., 2009. The boundless carbon cycle. Nat. Geosci. 2, 598–600.
Bauer, J., Bianchi, T., 2011. Author's personal copy 5.02 dissolved organic carbon cycling and transformation. Treatise Estuar. Coast. Sci. 5, 7–68.
Berhe, A.A., Harte, J., Harden, J.W., Torn, M.S., 2007. The significance of the erosion-induced terrestrial carbon sink. BioScience 57, 337.
Ciais, P., Sabine, C., Bala, G., Bopp, L., Brovkin, V., Canadell, J., Chhabra, A., Defries, R., Galloway, J., Heimann, M., 2014. Carbon and Other Biogeochemical Cycles. Climate Change 2013: the Physical Science Basis. Contribution of Working Group I to the Fifth Assessment Report of the Intergovernmental Panel on Climate Change. Cambridge University Press.
Cole, J.J., Prairie, Y.T., Caraco, N.F., McDowell, W.H., Tranvik, L.J., Striegl, R.G., Duarte, C.M., Kortelainen, P., Downing, J.A., Middelburg, J.J., 2007. Plumbing the global carbon cycle: integrating inland waters into the terrestrial carbon budget. Ecosystems 10, 172–185.
Da Silva Dias, R., De Abreu, C.A., De Abreu, M.F., Paz-Ferreiro, J., Matsura, E.E., Paz González, A., 2013. Comparison of methods to quantify organic carbon in soil samples from São Paulo State, Brazil. Commun. Soil Sci. Plant Anal. 44, 429–439.
Del Grosso, S., Parton, W., Mosier, A., Hartman, M., Brenner, J., Ojima, D., Schimel, D., 2001. Simulated interaction of carbon dynamics and nitrogen trace gas fluxes using the DAYCENT model. Modeling Carbon and Nitrogen Dynamics for Soil Management, pp. 303–332.
Devanand, M., Kyle, R.M., Shilpa, A., Keith, A.J., Gary, M.P., 2006. Calibration and validation of SWAT for field-scale sediment-yield prediction. In: 2006 ASAE Annual Meeting.
Donovan, P., 2012. Measuring soil carbon change. A Flexible, Practical, Local Method.
Ellison, W., 1947. Soil erosion studies—part I. Agric. Eng. 28, 145–146.
Gassman, P.W., Reyes, M.R., Green, C.H., Arnold, J.G., 2007. The soil and water assessment tool: historical development, applications, and future research directions. Trans. ASABE 50, 1211–1250.
Gelfand, I., Sahajpal, R., Zhang, X., Izaurralde, R.C., Gross, K.L., Robertson, G.P., 2013. Sustainable bioenergy production from marginal lands in the US Midwest. Nature 493, 514–517.
Gijsman, A.J., Hoogenboom, G., Parton, W.J., Kerridge, P.C., 2002. Modifying DSSAT crop models for low-input agricultural systems using a soil organic matter–residue module from CENTURY. Agron. J. 94, 462–474.
Grosz, B., Dechow, R., Gebbert, S., Hoffmann, H., Zhao, G., Constantin, J., Raynal, H., Wallach, D., Coucheney, E., Lewan, E., 2017. The implication of input data aggregation on up-scaling soil organic carbon changes. Environ. Model. Software 96, 361–377.
Gupta, H.V., Sorooshian, S., Yapo, P.O., 1999. Status of automatic calibration for hydrologic models: comparison with multilevel expert calibration. J. Hydrol. Eng. 4, 135–143.
Hao, Y., Lal, R., Izaurralde, R.C., Ritchie, J.C., Owens, L.B., Hothem, D.L., 2001. Historic assessment of agricultural impacts on soil and soil organic carbon erosion in an Ohio watershed. Soil Sci. 166, 116–126.
Hao, Y., Lal, R., Owens, L., Izaurralde, R., Post, W., Hothem, D., 2002. Effect of cropland management and slope position on soil organic carbon pool at the North Appalachian experimental watersheds. Soil Tillage Res. 68, 133–142.
Harden, J., Sharpe, J., Parton, W., Ojima, D., Fries, T., Huntington, T., Dabney, S., 1999. Dynamic replacement and loss of soil carbon on eroding cropland. Global Biogeochem. Cycles 13, 885–901.
Hoffmann, U., Hoffmann, T., Jurasinski, G., Glatzel, S., Kuhn, N., 2014. Assessing the spatial variability of soil organic carbon stocks in an alpine setting (Grindelwald, Swiss Alps). Geoderma 232, 270–283.
Hope, D., Billett, M., Cresser, M., 1994. A review of the export of carbon in river water: fluxes and processes. Environ. Pollut. 84, 301–324.
Houghton, R., 2002. Terrestrial carbon sinks–uncertain. Biologist 49.

IPCC, 2013. In: Stocker, T., Qin, D., Plattner, G.-K., Tignor, M., Allen, S.K., Boschung, J., Nauels, A., Xia, Y., V., B., Midgley, P.M. (Eds.), The Physical Science Basis. Contribution of Working Group I to the Fifth Assessment Report of the Intergovernmental Panel on Climate Change. Cambridge, United Kingdom and New York, NY, USA.

Izaurralde, R., Williams, J.R., McGill, W.B., Rosenberg, N.J., Jakas, M.Q., 2006. Simulating soil C dynamics with EPIC: model description and testing against long-term data. Ecol. Model. 192, 362–384.

Izaurralde, R., Williams, J.R., Post, W.M., Thomson, A.M., McGill, W.B., Owens, L., Lal, R., 2007. Long-term modeling of soil C erosion and sequestration at the small watershed scale. Climatic Change 80, 73–90.

Jeong, J., Kannan, N., Arnold, J., Glick, R., Gosselink, L., Srinivasan, R., Harmel, R., 2011. Development of sub-daily erosion and sediment transport algorithms for SWAT. Trans. ASABE 54, 1685–1691.

Jetten, V., De Roo, A., Favis-Mortlock, D., 1999. Evaluation of field-scale and catchment-scale soil erosion models. Catena 37, 521–541.

Jones, C., Dyke, P., Williams, J., Kiniry, J., Benson, V., Griggs, R., 1991. EPIC: an operational model for evaluation of agricultural sustainability. Agric. Syst. 37, 341–350.

Jones, J.W., Hoogenboom, G., Porter, C.H., Boote, K.J., Batchelor, W.D., Hunt, L., Wilkens, P.W., Singh, U., Gijsman, A.J., Ritchie, J.T., 2003. The DSSAT cropping system model. Eur. J. Agron. 18, 235–265.

Kelly, G.E., 1975. Soils of the North Appalachian Experimental Watershed. US Department of Agriculture, Agricultural Research Service.

Knisel, W.G., 1980. CREAMS: a Field Scale Model for Chemicals, Runoff, and Erosion from Agricultural Management Systems [USA]. Dept. of Agriculture. Conservation research report (USA), United States.

Lal, R., 2003. Soil erosion and the global carbon budget. Environ. Int. 29, 437–450.

Lal, R., 2004. Soil carbon sequestration impacts on global climate change and food security. Science 304, 1623–1627.

LeDuc, S.D., Zhang, X., Clark, C.M., Izaurralde, R.C., 2016. Cellulosic feedstock production on Conservation Reserve Program land: potential yields and environmental effects. GCB Bioenergy 9 (2), 460–468.

Legates, D.R., McCabe, G.J., 1999. Evaluating the use of "goodness-of-fit" measures in hydrologic and hydroclimatic model validation. Water Resour. Res. 35, 233–241.

Liu, S., Bliss, N., Sundquist, E., Huntington, T.G., 2003. Modeling carbon dynamics in vegetation and soil under the impact of soil erosion and deposition. Global Biogeochem. Cycles 17.

Luzio, M., Srinivasan, R., Arnold, J.G., 2002. Integration of watershed tools and SWAT model into BASINS. JAWRA J. Am. Water Resour. Assoc. 38, 1127–1141.

Menzel, R., 1980. Enrichment Ratios for Water Quality Modeling. CREAMS: A Field-Scale Model for Chemicals, Runoff, and Erosion from Agricultural Management Systems Conservation Research Report Number 26, May, 1980, pp. 486–492, 1 Fig, 2 Tab, 11 Ref.

Morgan, R., Quinton, J., Smith, R., Govers, G., Poesen, J., Auerswald, K., Chisci, G., Torri, D., Styczen, M., 1998. The European Soil Erosion Model (EUROSEM): a dynamic approach for predicting sediment transport from fields and small catchments. Earth Surf. Process. Landforms 23, 527–544.

Moriasi, D.N., Arnold, J.G., Van Liew, M.W., Bingner, R.L., Harmel, R.D., Veith, T.L., 2007. Model evaluation guidelines for systematic quantification of accuracy in watershed simulations. Trans. ASABE 50, 885–900.

Müller-Nedebock, D., Chaplot, V., 2015. Soil carbon losses by sheet erosion: a potentially critical contribution to the global carbon cycle. Earth Surf. Process. Landforms 40, 1803–1813.

Nash, J.E., Sutcliffe, J.V., 1970. River flow forecasting through conceptual models part I—a discussion of principles. J. Hydrol. 10, 282–290.

Nearing, M., Foster, G., Lane, L., Finkner, S., 1989. A process-based soil erosion model for USDA-Water Erosion Prediction Project technology. Trans. ASAE 32, 1587–1593.

Nearing, M., Jetten, V., Baffaut, C., Cerdan, O., Couturier, A., Hernandez, M., Le Bissonnais, Y., Nichols, M., Nunes, J., Renschler, C., 2005. Modeling response of soil erosion and runoff to changes in precipitation and cover. Catena 61, 131–154.

Neitsch, S.L., Arnold, J.G., Kiniry, J.R., Williams, J.R., 2011. Soil and Water Assessment Tool Theoretical Documentation Version 2009. Texas Water Resources Institute.

Nord, G., Esteves, M., 2005. PSEM_2D: a physically based model of erosion processes at the plot scale. Water Resour. Res. 41.

Owens, L., Bonta, J., Shipitalo, M., 2010. USDA-ARS North Appalachian Experimental Watershed: 70-year hydrologic, soil erosion, and water quality database. Soil Sci. Soc. Am. J. 74, 619–623.

Owens, L.B., Edwards, W.M., 1993. Tillage studies with a corn-soybean rotation: Surface runoff chemistry. Soil Sci. Soc. Am. J. 57 (4), 1055–1060.

Park, S., Mitchell, J., Scarborough, J., 1982. Soil erosion simulation on small watersheds: a modified ANSWERS model. Trans. ASAE 25, 1581–1588.

Parton, W., Scurlock, J., Ojima, D., Gilmanov, T., Scholes, R., Schimel, D.S., Kirchner, T., Menaut, J.C., Seastedt, T., Garcia Moya, E., 1993. Observations and modeling of biomass and soil organic matter dynamics for the grassland biome worldwide. Global Biogeochem. Cycles 7, 785–809.

Parton, W.J., Ojima, D.S., Cole, C.V., Schimel, D.S., 1994. A general model for soil organic matter dynamics: sensitivity to litter chemistry, texture and management. In: Quantitative Modeling of Soil Forming Processes, pp. 147–167. SSSA Spec. Public No. 39.

Quinton, J.N., Govers, G., Van Oost, K., Bardgett, R.D., 2010. The impact of agricultural soil erosion on biogeochemical cycling. Nat. Geosci. 3, 311–314.

Renard, K.G., Foster, G.R., Weesies, G.A., Porter, J.P., 1991. RUSLE: revised universal soil loss equation. J. Soil Water Conserv. 46, 30–33.

Richardson, C., Bucks, D., Sadler, E., 2008. The conservation effects assessment project benchmark watersheds: synthesis of preliminary findings. J. Soil Water Conserv. 63, 590–604.

Schumacher, B.A., 2002. Methods for the Determination of Total Organic Carbon (TOC) in Soils and Sediments. Ecological Risk Assessment Support Center, pp. 1–23.

Shipitalo, M.J., Edwards, W.M., 1998. Runoff and erosion control with conservation tillage and reduced-input practices on cropped watersheds. Soil Tillage Res. 46 (1–2), 1–12.

Smith, S., Renwick, W., Buddemeier, R., Crossland, C., 2001. Budgets of soil erosion and deposition for sediments and sedimentary organic carbon across the conterminous United States. Global Biogeochem. Cycles 15, 697–707.

Srinivasan, R., Zhang, X., Arnold, J., 2010. SWAT ungauged: hydrological budget and crop yield predictions in the Upper Mississippi River Basin. Trans. ASABE 53, 1533–1546.

Stallard, R.F., 1998. Terrestrial sedimentation and the carbon cycle : coupling weathering and erosion to carbon burial. Global Biogeoch. 12, 231–257.

Tank, J., Rosi-Marshall, E., Griffiths, N.A., Entrekin, S.A., Stephen, M.L., 2010. A review of allochthonous organic matter dynamics and metabolism in streams. J. North Am. Benthol. Soc. 29, 118–146.

Tilman, D., Hill, J., Lehman, C., 2006. Carbon-negative biofuels from low-input high-diversity grassland biomass. Science 314, 1598–1600.

Tranvik, L.J., Downing, J.A., Cotner, J.B., Loiselle, S.A., Striegl, R.G., Ballatore, T.J., Dillon, P., Finlay, K., Fortino, K., Knoll, L.B., 2009. Lakes and reservoirs as regulators of carbon cycling and climate. Limnol. Oceanogr. 54, 2298–2314.

Trimmer, M., Grey, J., Heppell, C.M., Hildrew, A.G., Lansdown, K., Stahl, H., Yvon-Durocher, G., 2012. River bed carbon and nitrogen cycling: state of play and some new directions. Sci. Total Environ. 434, 143–158.

Van Oost, K., Quine, T.A., Govers, G., De Gryze, S., Six, J., Harden, J.W., Ritchie, J.C., McCarty, G.W., Heckrath, G., Kosmas, C., Giraldez, J.V., Da Silva, J.R.M., Merckx, R., 2007. The impact of agricultural soil erosion on the global carbon cycle. Science (New York, N.Y.) 318, 626–629.

Walter, K., Don, A., Tiemeyer, B., Freibauer, A., 2016. Determining soil bulk density for carbon stock calculations: a systematic method comparison. Soil Sci. Soc. Am. J. 80, 579–591.

Wang, Z., Govers, G., Oost, K.V., Clymans, W., Putte, A.V., Merckx, R., 2013. Soil organic carbon mobilization by interrill erosion: insights from size fractions. J. Geophys. Res. Earth Surface 118, 348–360.

Williams, J., Berndt, H., 1977. Sediment yield prediction based on watershed hydrology. Trans. ASAE 20, 1100–1104.

Williams, J., Jones, C., Kiniry, J., Spanel, D.A., 1989. The EPIC crop growth model. Trans. ASAE (USA) 32 (2), 497–511.

Williams, J.R., 1990. The erosion-productivity impact calculator (EPIC) model: a case history. Phil. Trans. Roy. Soc. Lond. B Biol. Sci. 329, 421–428.

Wischmeier, W.H., Smith, D.D., 1978. Predicting rainfall erosion losses-a guide to conservation planning. Predicting Rainfall Erosion Losses-a Guide to Conservation Planning.

Wischmeir, W.H., 1965. Predicting Rainfall-erosion Losses from Cropland East of the Rocky Mountain, Guide for Selection of Practices for Soil and Water Conservation. Agricultural Handbook, p. 282.

Woods, L., Schuman, G., 1988. Cultivation and slope position effects on soil organic matter. Soil Sci. Soc. Am. J. 52, 1371–1376.

Woolhiser, D., Smith, R., Goodrich, D., 1990. KINEROS. A Kinematic Runoff and Erosion Model. Documentation and User Manual, ARS-77.

Wu, Y., Liu, S., Qiu, L., Sun, Y., 2016. SWAT-DayCent coupler: an integration tool for simultaneous hydro-biogeochemical modeling using SWAT and DayCent. Environ. Model. Software 86, 81–90.

Yang, Q., Zhang, X., 2016. Improving SWAT for simulating water and carbon fluxes of forest ecosystems. Sci. Total Environ. 569, 1478–1488.

Yang, Q., Zhang, X., Abraha, M., Del Grosso, S., Robertson, G., Chen, J., 2017. Enhancing the soil and water assessment tool model for simulating N2O emissions of three agricultural systems. Ecosys. Health Sustain. 3.

Zhang, X., Beeson, P., Link, R., Manowitz, D., Izaurralde, R.C., Sadeghi, A., Thomson, A.M., Sahajpal, R., Srinivasan, R., Arnold, J.G., 2013a. Efficient multi-objective calibration of a computationally intensive hydrologic model with parallel computing software in Python. Environ. Model. Software 46, 208–218.

Zhang, X., Izaurralde, R.C., Arnold, J.G., Williams, J.R., Srinivasan, R., 2013b. Modifying the soil and water assessment tool to simulate cropland carbon flux: model development and initial evaluation. Sci. Total Environ. 463, 810–822.

Zhang, X., Izaurralde, R.C.S., Arnold, J.G., Sammons, N.B., Manowitz, D.H., Thomson, A.M., Williams, J.R., 2011. Comment on "modeling Miscanthus in the soil and water assessment tool (SWAT) to simulate its water quality effects as a bioenergy crop". Environ. Sci. Technol. 45, 6211–6212.

Zhang, X., Sahajpal, R., Manowitz, D.H., Zhao, K., LeDuc, S.D., Xu, M., Xiong, W., Zhang, A., Izaurralde, R.C., Thomson, A.M., 2014. Multi-scale geospatial agro-ecosystem modeling: a case study on the influence of soil data resolution on carbon budget estimates. Sci. Total Environ. 479, 138–150.